Journal of Catalysis **189,** 158–169 (2000)
doi:10.1006/jcat.1999.2681, available online at http://www.idealibrary.com on IDEAL®

Qualitative Evidence for Adsorbate-Induced Edge Metal Atom Localization: The Characterization of Lifted Backbond Degeneracy in Adsorbed CO through the Model Adsorption of Methyl Isocyanide on Pd/Al_2O_3

Mark R. Albert[1]

Surface Science Center, Department of Chemistry, University of Pittsburgh, Pittsburgh, Pennsylvania 15260

Received June 17, 1999; revised September 3, 1999; accepted September 10, 1999

Qualitative synthetic chemistry strategies are used to show that electron-deficient (i.e., unstable) edge Pd atoms can find stability through separation from the surface band structure and strong bonding to a CO adsorbate state that displays lifted backbond degeneracy. This conclusion is drawn from the transmission infrared observation of a thermally activated bonding mode of CO on Pd/Al_2O_3 that has characteristics inconsistent with conventional atop- or bridge-bonded CO but similarities with an "atop bent" methylisocyanide adsorbate mode, characterized on the same surface, which is known to have lifted backbond degeneracy. Analysis of qualitative observations in both the data and the literature indicates the thermally stable CO state to be atop bound to an edge atom. Since this state is populated over a wide temperature range, the ΔH for its formation must arise from the attached surface metal atom gaining stability in the process even at the expense of CO stability. Published work [*J. Phys. Chem.* 93, 4890 (1989); *Phys. Rev. B* 24, 754 (1981)] indicates that unstable edge atoms are the likely candidates for that behavior. A TLEED study [*Chem. Phys. Lett.* 201, 393 (1993)] that reports the identical CO adsorbate state on Pd(110) and a study reporting the ability of adsorbed CO to reconstruct the Pd(110) surface [*Chem. Phys. Lett.* 167, 391 (1990); *Surf. Sci.* 249, 1 (1991)] are published observations that are consistent with this conclusion.

Key Words: **infrared absorption spectroscopy; chemisorption; surface chemical reaction; palladium; carbon monoxide; methylisocyanide; lifted backbond degeneracy.**

I. INTRODUCTION

Determination of the mechanisms of heterogeneously catalyzed reactions remains one of the major challenges of surface science and catalysis (1–5). This is due in large part to difficulty detecting surface intermediates that have short lifetimes or low steady-state surface concentrations (6, 7). However, since the organometallic chemistry literature reports a wide range of structures for numerous ligands (8, 9), the possibility exists that one or more of these unusual ligand bonding modes might qualitatively represent intermediate states in heterogeneous catalytic reactions. Pursuit of adsorbates that mimic these ligand states, therefore, could offer insight into the mechanisms of heterogeneous catalytic reactions.

One diatomic adsorbate state that workers have only recently begun to pursue (10–13) and is not usually a focus of theoretical studies (14–17) arises from the possibility that the degeneracy of the two backbonding molecular orbitals of adsorbed CO could be lifted with chemisorption. This would result in an "atop"-bound CO that has both a double carbon–oxygen bond and a double metal–carbon bond **(III)** (described in Section IV.A). Since the bond order of the CO adsorbate is reduced from 3 to 2 in this state, it could be an intermediate in CO reduction (18), scission (2), or oxidation (19). While this "lifted backbond degeneracy" adsorbate state has not been specifically reported for coordinated CO, it has been characterized in a ligand state for the analogous methylisocyanide **(I)** ligand (20).

$$:C\equiv N-CH_3$$

(I)

Previous studies of methylisocyanide **(I)** adsorbed on supported metals (21–23), single crystals (24–29), and gold powder (30) have already suggested that qualitative similarities in adsorbate bonding exist between it and adsorbed CO and these similarities are consistent with a theoretical work (31) that has generalized the bonding of all diatomic ligands in complexes into a series of predictable electronic effects. It is therefore not unreasonable to presume a generally similar situation on surfaces (9, 32).

One reason that a lifted backbond degeneracy CO coordination mode has not been reported in the organometallic chemistry literature may be that the physical differences between the conventional CO adsorbate state with degenerate backbonds **(II)** and the speculated CO adsorbate state with "lifted backbond degeneracy" **(III)** are likely quite small

[2] mralbert@netaxs.com

0021-9517/00 $35.00

and so would be difficult to distinguish by standard analytical methods. A similar situation would exist for surface analysis.

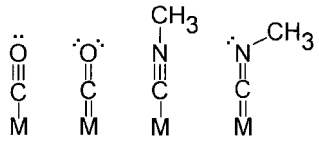

(II) (III) (IV) (V)

But since the lifted backbond degeneracy state has been reported for coordinated methylisocyanide **(V)** (20), it is possible to study methylisocyanide adsorption as a model of CO adsorption. If adsorbed methylisocyanide is found to have an adsorbate mode that displays the "atop bent" state with its lifted backbond degeneracy (Section IV.A), it will become possible to compare the characteristics of that mode with those of detectable CO states on the same surface to determine if, in conjunction with literature reports, any of those CO states can be identified as having lifted backbond degeneracy. This report includes the results of just such a model study on the Pd/Al_2O_3 surface.

This methodology can be considered an expansion of the cross-disciplinary approach known as the "cluster-surface analogy" (9, 33, 34) that would meld the research strategies of surface science with those of both organometallic and synthetic chemistry. However, its application of organometallic and synthetic chemistry research approaches to surface systems may cause confusion since certain of its viewpoints differ from those of engineering, physical chemistry, or physics.

For instance, a qualitative model study must accommodate an inherently large experimental error since a model cannot duplicate the molecule being studied. However, the study can still yield new information if it focuses on broad conclusions that are significant relative to that large error. This excludes many important issues but allows for the study of general concepts that can focus future efforts. This large error also allows for simplified data acquisition and analysis since experimental error in one aspect of the study cannot be improved by higher accuracy in an another.

A second source of confusion may lie with the qualitative characterization strategies used in this work. Unlike physical chemistry studies that seek out direct measurements to assign adsorbate structures, and unlike a mathematical proof, qualitative characterization of a molecular structure (35) requires only that a limited number of possible outcomes be reduced to one. This is done by finding contradictions between the data and candidate structures until all possible structures are eliminated except one.

II. EXPERIMENTAL

All spectra were collected using a purged Perkin–Elmer infrared spectrophotometer (Model PE-783) employing a slit program yielding a resolution of 5.4 cm^{-1}. Computer-assisted data acquisition allowed the use of signal averaging to improve the signal-to-noise ratio of all data collected as well as the subtraction of background effects associated with both the clean and adsorbate-covered alumina support.

Both the Pd/Al_2O_3 and alumina-only substrate were prepared and supported on a single CaF_2 disk in the infrared beam in a high-vacuum cell with CaF_2 windows as described previously (36); the window transmission allowed spectral analyses in the range 4000 to 1050 cm^{-1}. Since the sample is supported on metal tubing, cold or hot flowing gas within the tubing allowed measurements to be made at any substrate temperature between 77 and 600 K.

The samples of dispersed palladium crystallites on alumina were prepared by a method described previously (36). The final Pd/Al_2O_3 preparation contained 9% by weight Pd in crystallites with an average size of 75 Å. This process usually left some adsorbed CO behind. This was removed by the addition of 8.5×10^{13} molecules of O_2 to the sample at 300 K followed by a 60-min hydrogen reduction at 450 K. After reduction, the sample was allowed to cool slowly under vacuum after a 1-h bake-out at 450 K.

Methylisocyanide was prepared by the dehydration of *N*-methylformamide (Aldrich) with excess P_2O_5 (Baker). This was accomplished through the dropwise addition of the formamide to an evacuated flask cooled in a dry ice bath containing the powdered P_2O_5. The ratio of the reactants was 140 g of *N*-methylformamide to 84 g of P_2O_5. The raw product contained a small amount of acetonitrile which was removed by vacuum distillation of the first few percent of the product at room temperature. The volatile methylisocyanide product was characterized by the presence of a methylisocyanide ν(CN) mode at 2150 cm^{-1} and the absence of an acetonitrile ν(CN) mode at 2267 cm^{-1} and stored in a sealed glass ampoule at 77 K. While the yield of this preparative route was low (~10%), its simplicity and low cost made it preferable to more efficient, and more complex, preparations (37). Spectroquality CO was taken from laboratory stock.

III. RESULTS

A. *Methylisocyanide Adsorption on Pd/Al_2O_3 at 190 K*

Figure 1 shows the transmission infrared spectra between 2300 and 1600 cm^{-1} of methylisocyanide adsorbed on palladium crystallites at 190 K. The data for five consecutive exposures of 1×10^{18} molecules of methylisocyanide are shown. The temperature 190 K was chosen as the minimum surface temperature since a previous study (21) revealed that lower temperatures made the methylisocyanide vapor preferentially condense on the copper sample support.

Three peaks develop with increasing exposure: a narrow peak at 2180 cm^{-1}, a broad peak skewed to lower energy and peaking at 2050 cm^{-1}, and a well-defined shoulder centered

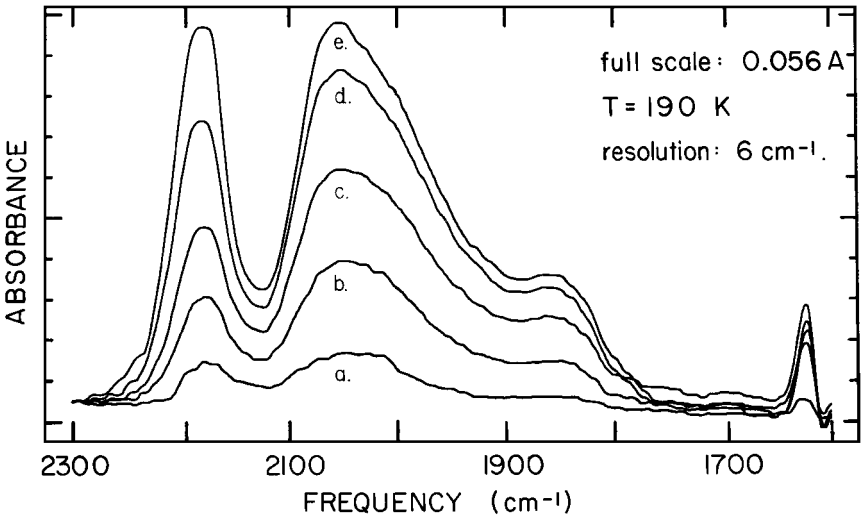

FIG. 1. Development of ν(CN) peaks on Pd/Al_2O_3 due to increasing methylisocyanide exposure at 190 K. Total exposures were (a) 1×10^{18}, (b) 2×10^{18}, (c) 3×10^{18}, (d) 4×10^{18}, and (e) 5×10^{18} molecules.

at 1850 cm^{-1}. These three peaks grow at approximately the same rate with increasing exposure, even though the narrow peak at 2180 cm^{-1} may have lagged somewhat behind the other two. Since the small, sharp feature at 1620 cm^{-1} has positive- and negative-going components, it must be due to an alumina-based peak that shifts with increasing methylisocyanide physisorption and causes an incomplete peak subtraction.

No indication of peak shifting with increasing coverage is detected in Fig. 1. This allows for the exclusion of dipole coupling effects that might lead to ambiguities in the peak assignments (38, 39). A report (40) describing the relatively small number of active sites on the Pd/Al_2O_3 surface is consistent with this observation since the active adsorption sites are less likely to be nearest neighbors on the dispersed metal.

B. Effect of Heating Chemisorbed Methylisocyanide

Figure 2 shows how the vibrational peaks described in Fig. 1 change as the sample is heated above 190 K in roughly 40 K steps to 352 K. Four changes are evident: (1) the narrow peak at 2180 cm^{-1} attenuates, (2) the broad peak with its maximum at 2050 cm^{-1} attenuates, (3) a broad peak develops around 1980 cm^{-1}, and (4) the small peak at 1850 cm^{-1} increases in intensity at about the same rate as the 1980 cm^{-1} peak and becomes a shoulder of that peak. Unusual for surface data (41), a sharp isosbestic point

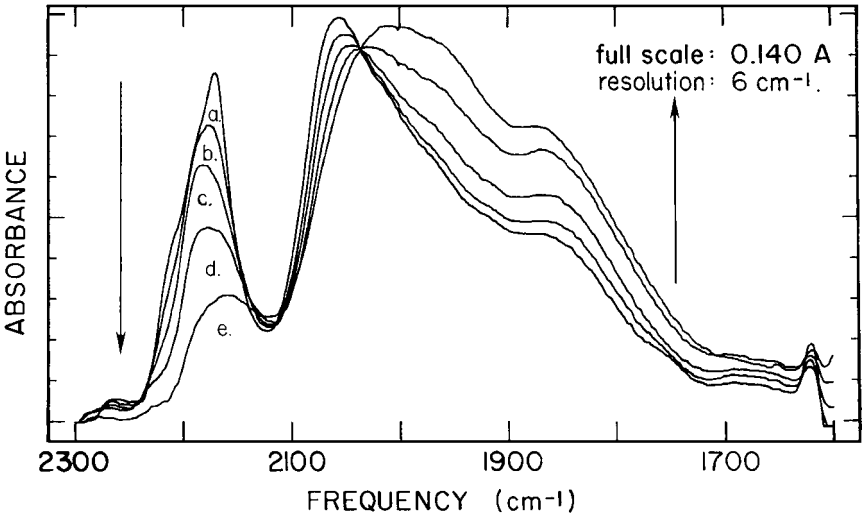

FIG. 2. Variation in the ν(CN) peaks for methylisocyanide adsorbed on Pd/Al_2O_3 after the sample temperature was momentarily increased to (a) 190 K, (b) 233 K, (c) 273 K, (d) 310 K, and (e) 352 K. An isosbestic point is apparent at 2035 cm^{-1}.

appears at 2035 cm^{-1} between the peaks at 2050 and 1980 cm^{-1}. The alumina-based structure at 1625 cm^{-1} also attenuates with increasing temperature.

Figure 3 shows the relative partial pressures of masses 2 (H_2), 27 (HCN), and 38 (methylisocyanide fragment) in the vacuum system as the saturated methylisocyanide overlayer is slowly heated from 200 to 500 K. No other peaks that could be associated with other gases such as cyanogen (mass 52) and methane (mass 16) were detected. For all temperatures, the HCN partial pressure (mass 27) follows that of the methylisocyanide fragment (mass 38) and indicates that the HCN peak is due only to fragmentation of methylisocyanide and not desorption of HCN. The partial pressure of hydrogen follows that of methylisocyanide up to around 400 K above which it increases while the methylisocyanide and HCN partial pressures drop off. This indicates the onset of methylisocyanide decomposition but at a temperature above the warmest annealing temperature used for the data collected in Fig. 2. The discontinuity at 300 K is caused by a shift in the mass spectrometer sensitivity required to keep the raw data on scale.

C. Thermal Processing of CO on Pd/Al_2O_3

Figure 4 illustrates how the IR spectrum of a saturated CO overlayer on Pd/Al_2O_3 evolves as the sample is heated above 95 K in roughly 40 K steps to 457 K. These data are qualitatively similar to those in Fig. 2. Three absorption peaks are visible near 2110, 1990, and 1925 cm^{-1}. Between 85 and 233 K the peak near 2110 cm^{-1} attenuates. The peak near 1990 cm^{-1} intensifies to a maximum but attenuates above 190 K as it shifts to lower frequency. During the entire range of thermal processing, the peak near 1925 cm^{-1} grows in intensity.

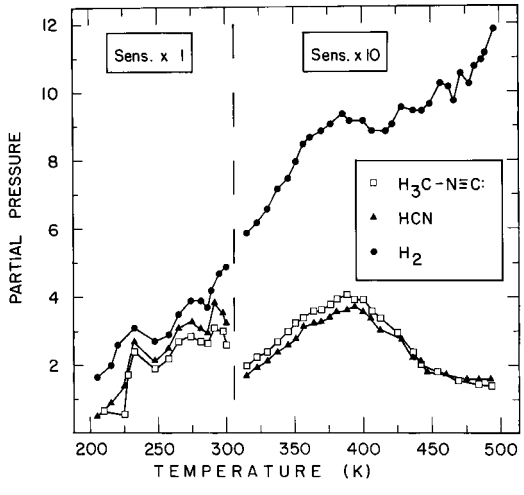

FIG. 3. Changes in the relative partial pressures of masses 2 (H_2), 27 (HCN), and 38 (methylisocyanide fragment) as a methylisocyanide overlayer on Pd/Al_2O_3 was heated under vacuum from 200 to 500 K.

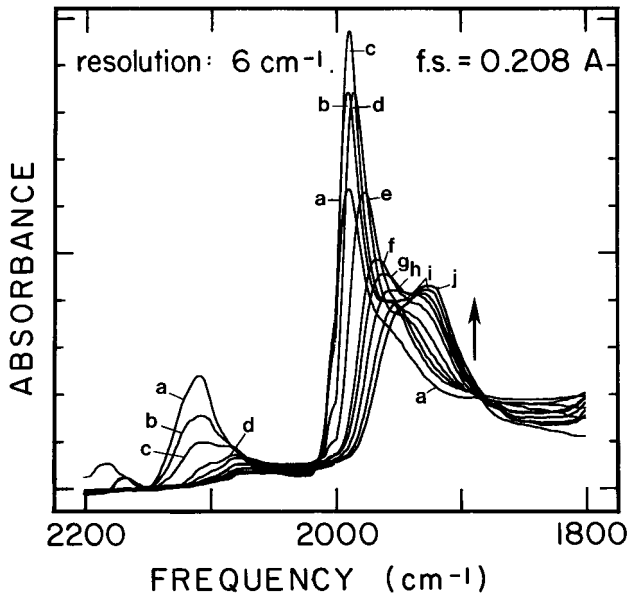

FIG. 4. Variation in the ν(CO) peaks for CO adsorbed on Pd/Al_2O_3 after the sample temperature was momentarily increased to (a) 95 K, (b) 140 K, (c) 190 K, (d) 233 K, (e) 273 K, (f) 310 K, (g) 347 K, (h) 384 K, (i) 419 K, and (j) 457 K.

While it might be expected that dipole coupling would shift the 1925 cm^{-1} peak to higher frequency as its associated adsorbate state is populated (38, 39), the peak at 1925 cm^{-1} initially shifts to lower frequency, then remains stationary. Close inspection indicates that it grows independently of the shifting 1990 cm^{-1} peak. Comparison of these data with exposure-dependent data for CO adsorbed on Pd/SiO_2 indicates that the described changes are not due to coverage dependence (41, 42).

IV. DISCUSSION

A. Valence Bond Description of Lifted Backbond Degeneracy in Diatomics and Its Detection in Methylisocyanide

As described previously (43–45), when the backbonding to a diatomic such as atop CO is either degenerate or nonexistent, both atoms of the diatomic retain the *sp* hybridization of gas-phase CO **(II)**. But if the backbond degeneracy were to be lifted, the bonding between the surface and CO molecule would evolve toward a "$\sigma + \pi$" double bond between the metal and carbon atom **(III)** and lead to double-bond formation between the carbon and oxygen atoms. The carbon atom would retain *sp* hybridization but the oxygen atom would lose one of its π bonds to the carbon atom, rehybridize into an sp^2 configuration and acquire a second lone electron pair on the oxygen atom.

Characterizing this transformation in CO experimentally, however, is difficult since the described electronic changes lead to only subtle variations in bond lengths and orbital structure. These changes would also lead to an ambiguous shift in the ν(CO) diatomic stretching frequency since coupling with the metal–carbon double bond would change the mode into a ν_{asym}(M=C=O) stretch that would have a frequency undefinable by the conventional methods used for assigning CO adsorbate modes to ν(CO) stretching frequencies (46, 47). Unambiguous characterization of lifted backbond degeneracy in adsorbed diatomics using vibrational methods, therefore, must be aided with the study of model adsorbates that display a much greater degree of detectable structural variability.

This can be done with methylisocyanide **(I)**. While its diatomic part (CN) qualitatively models CO (9, 21, 31, 32), its methyl group will tilt its C_{3v} axis away from the CN axis as the backbond degeneracy lifts to accommodate the appearance of the lone electron pair on the nitrogen atom **(V)** (43–45). Characterization of this methyl group tilting, therefore, offers an indirect, though unambiguous, method for detecting lifted backbond degeneracy in the "diatomic" CN part of adsorbed methylisocyanide.

Within organometallic chemistry, this methyl group tilting has already been indirectly applied to the characterization of lifted backbond degeneracy in coordinated methylisocyanide since crystallography has been used to characterize a wide variety of methylisocyanide ligand coordination modes. This has allowed for the facile correlation of ν(CN) vibrational energies to a wide variety of methylisocyanide ligand structures with methyl group axes both aligned with and tilted away from the CN axis (Fig. 5) (24, 43). Since summaries of this work show that the ν(CN) vibrational energies of these bonding modes are widely spaced (Fig. 5), the characterization of methylisocyanide ligand structure from vibrational data becomes a straightforward activity and includes the direct characterization of backbond degeneracy. And, since these correlations have already been used to characterize methylisocyanide adsorbate structures (21–27), the same data summaries can also be applied to characterize backbond degeneracy in the present model study of methylisocyanide adsorbed on Pd/Al_2O_3.

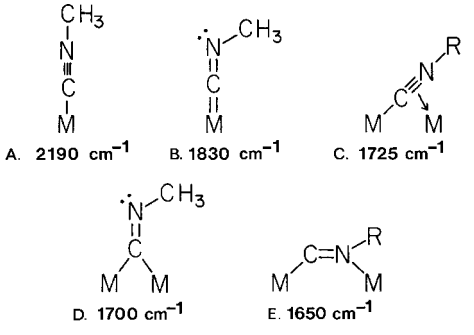

FIG. 5. Five ligand bonding modes, and their corresponding ν(CN) stretching frequencies (24), for coordinated methylisocyanide in metal complexes: (A) atop linear, (B) atop bent, (C) σ–π bridge, (D) bent bridge, and (E) flat-lying bridge coordination modes.

B. Characterization of Methylisocyanide Adsorbate Modes on Pd/Al_2O_3

Methylisocyanide adsorption has been studied using vibrational methods on Rh(111) (21), Rh/Al_2O_3 (22), Ag(311) (27), Pt/SiO_2 (23), Pt(111) (24, 26), and Ni(111) (25). Of the methylisocyanide ligand bonding modes found in metal complexes (Fig. 5) (24), the most commonly identified adsorbate mode is the "atop linear" mode (Fig. 5A) associated with a ν(CN) stretching frequency of 2190 cm^{-1} (24). All clean surfaces are reported to display this adsorbate mode (21–27). Rh/Al_2O_3 (22) and Ag(311) (27) data show only the peak associated with this "atop linear" mode, while the other systems (21, 23–26) also show a peak near 1700 cm^{-1} which is assigned to the "bridge bent" methylisocyanide mode (Fig. 5D). The "flat-lying bridge" bonding mode (Fig. 5E) cannot be unambiguously excluded as an assignment for this peak but is considered unlikely since no ν(C–H) vibration softening is detected (22) that would indicate the expected hydrogen–surface interaction. No reliance on isotopic labeling is used in making any of these assignments and data such as additional vibrational peaks, TPD or ESDIAD, play a lesser corroborative role.

Based on these precedents (21–27), therefore, the peak detected at 2180 cm^{-1} in this work (Fig. 1) can be assigned to the "atop linear" mode (Fig. 5A) (24, 43) since it is red shifted only 10 cm^{-1} relative to that of the "atop linear" mode found in metal complexes. The possibility that this or any of the peaks in Fig. 1 may be due to a CN^- adsorbate can be excluded since no HCN is seen to desorb from the surface (Fig. 3), the scission of a H_3C–N single bond is disfavored on Pd(111) (48, 49), and the vibrational data for adsorbed cyanide on Pd differ from those shown in Fig. 1 (50).

Peaks near 1850 cm^{-1} such as that seen in Fig. 1 have previously been reported only for methylisocyanide adsorbed on precovered surfaces such as Rh(111) with preadsorbed CO or oxygen (22) and Ni(111) with preadsorbed carbon (25). In these cases, surface deactivation by the coadsorbate was believed to weaken the interaction of the "bridge bent" (Fig. 5D) methylisocyanide adsorbate and move its associated ν(CN) frequency to higher energy (22).

Since the Pd/Al_2O_3 surface in this study is clean, the peak at 1850 cm^{-1} can be assigned to the "atop bent" methylisocyanide mode (Fig. 5B) (24, 43) because its associated frequency is only 20 cm^{-1} higher than the ν(CN) stretching frequency found for the "atop bent" mode in metal complexes.

The peak near 2050 cm^{-1} in Fig. 1 does not correlate with the commonly reported methylisocyanide ligand bonding modes of Fig. 5. However, a linear methylisocyanide ligand bridge bonded in a threefold hollow site, with a stretching

frequency at 1943 cm^{-1}, has been found by X-ray crystallography in a triangular nickel cluster (51). Since the peak in Fig. 1 lies 100 cm^{-1} to higher energy than this reported threefold bound ligand, the associated bonding mode on Pd/Al_2O_3 is likely a "bridge linear" mode but only doubly bridged to account for the smaller red shift (52).

While the peak growing in at 1980 cm^{-1} (Fig. 2) might be assigned to the threefold "bridge linear" methylisocyanide mode (51), a more likely interpretation arises from examination of the IR spectrum of the compound methylisothiocyanate **(VI)** (53, 54), a structural analog of adsorbed methylisocyanide's "atop bent" mode (Fig. 5B) already assigned to the peak at 1850 cm^{-1} (its sulfur atom would model the metal atom). This IR spectrum reveals that methylisothiocyanate displays an overtone lying on the high-frequency side of its own ν(CN) absorption peak [rigorously the ν_{asym}(SCN) mode]. This overtone has been assigned to the ν_{svm}(SCN) fundamental (53, 54). Alkyl selenocyanates show similar vibrational data (55). This overtone can be as intense as or more intense than the ν_{asym}(SCN) mode due to a Fermi resonance interaction with the ν_{asym}(SCN) mode (53). Although shifted to a lower frequency, likely due to association with the metal surface, a similar assignment of the peak at 1980 cm^{-1} (Fig. 2) is a likely possibility for the "atop bent" methylisocyanide adsorbate mode, especially since its peak at 1850 cm^{-1} grows with thermal processing at about the same rate. A similar peak is reported, though not assigned, for a metal complex containing an "atop bent" methylisocyanide ligand (20).

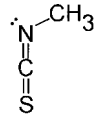

(VI)

The peak assignments discussed above are summarized in Fig. 6.

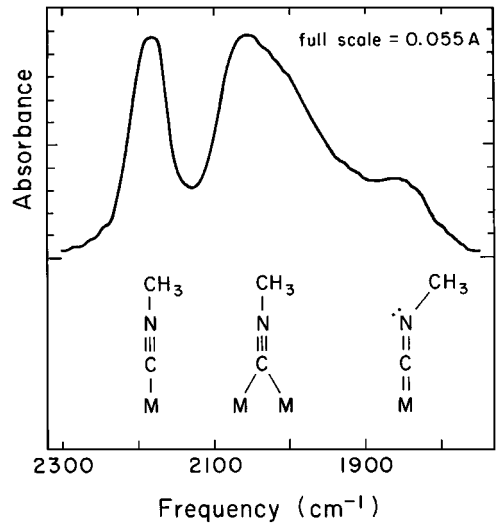

FIG. 6. Summary of ν(CN) peak assignments for methylisocyanide adsorbed on Pd/Al_2O_3. The peak at 2180 cm^{-1} is assigned to the "atop linear" mode; the peak at 2050 cm^{-1}, the "bridge linear" mode; and the shoulder centered at 1850 cm^{-1}, the "atop bent" mode.

C. Behavior of Methylisocyanide Adsorbate Modes with Thermal Processing

The data shown in Fig. 2 indicate how the three methylisocyanide bonding modes associated with the four peaks in the region between 2300 and 1600 cm^{-1} behave with thermal processing. First, since both peaks at 2180 and 2050 cm^{-1} attenuate with increasing temperature, both the "atop linear" and "bridge linear" modes of adsorbed methylisocyanide are removed from the surface as the temperature is raised. Second, since both peaks at 1980 and 1850 cm^{-1} grow with sample heating, the "atop bent" mode is populated with increasing temperature. Since all data collection took place at low temperature after annealing, the "atop bent" structure does not decay at lower temperatures.

The sharp isosbestic point at 2035 cm^{-1} that falls between the peaks at 2050 and 1980 cm^{-1} clearly indicates that the "atop bent" adsorbate mode is being prepared quantitatively from the "bridge linear" mode since the peak at 1980 cm^{-1} is likely associated with the "atop bent" mode. The "atop linear" mode associated with the peak at 2180 cm^{-1} must, therefore, associatively desorb from the surface with increasing surface temperature (Fig. 2), consistent with the mass spectral data in Fig. 3.

D. Characterization of Lifted Backbond Degeneracy in Adsorbed CO

1. Interpretation of model methylisocyanide data. Based on the valence bond arguments presented in Section IV.A, the IR data indicate that one of the methylisocyanide adsorbate modes on Pd/Al_2O_3, the "atop bent" mode (Fig. 5B) described by a ν(CN) peak at 1850 cm^{-1} (Fig. 2), displays lifted backbond degeneracy (43–45). The resulting metal–carbon double bond requires that the mode's ν(CN) stretch be correctly labeled as the ν_{asym}(M=C=N) stretch mode. It might be pointed out, therefore, that the 340 cm^{-1} red shift of this vibration relative to that of gas-phase methylisocyanide occurs for a reason unrelated to site coordination as first proposed by Eischens *et al.* (52) for CO adsorption and so is an alternate explanation for the red shift seen for one of methylisocyanide's "ν(CN)" vibrational peaks (9, 32).

This model result makes it worthwhile to explore the data for CO on Pd/Al_2O_3 to determine if the red shifts of some of its vibrational peaks might also be due, in retrospect, to adsorbate modes with lifted backbond degeneracy **(III)** instead of site coordination. This can be done by first determining if any vibrational peaks for adsorbed CO on

Pd/Al_2O_3 behave like the peaks seen for the "atop bent" methylisocyanide mode **(V)**.

Therefore, it can be concluded from the data that the "atop bent" adsorption mode of methylisocyanide on Pd/Al_2O_3 is prepared by thermal activation of a degenerately backbonded bridging adsorbate mode and displays a vibrational peak on the low-energy side of the bridge bond region of the "diatomic" adsorbate. Vibrational peaks of adsorbed CO having these characteristics, therefore, would become candidates for further consideration as having lifted backbond degeneracy.

While the above data acquisition (56) and interpretation for the methylisocyanide system may be judged incomplete according to established surface science standards, the inherently limited ability of methylisocyanide to model adsorbed CO cannot be improved upon by a more detailed analysis. Since the above information drawn from the model system turns out to be quite limited, the data interpretation is adequate for the present application.

2. Interpretation of the CO adsorption data. That thermal activation may be significant in the characterization of lifted backbond degeneracy limits the search for a lifted backbond degeneracy CO mode since few studies of CO chemisorption present thermal processing studies above 300 K even when TPD data show more peaks above room temperature than there are characterized states at room temperature (42, 57–61). This may not be surprising since the possibility of finding thermally populated CO adsorbate states above 300 K has not generally been considered (46, 47) prior to this model methylisocyanide study.

Only one paper could be found describing the effects of thermal processing on CO adsorbed on supported Pd above 300 K in a vacuum (62). In this work, the authors compared coverage-dependent CO vibrational data on Pd/SiO_2 after preparing the overlayers by both stepwise exposure at 300 K and stepwise desorption through thermal processing above 300 K. The two sets of data differ significantly and so could indicate a thermal processing impact on the adsorbed CO even though this was not the authors' interpretation (62).

The more detailed thermal processing data for CO on Pd/Al_2O_3 shown in Fig. 4 are consistent with this report (62) and one other (63). Additional reports show similar data (64–67) but in the presence of background CO where the results vary somewhat. These reports and others (41, 68–73) have consistently assigned the peaks at 2110 and 1990 cm^{-1} (Fig. 4) to atop- and bridge-bound CO, respectively, on both single-crystal palladium surfaces and supported palladium. Exceptions include recent photoelectron diffraction (74, 75) and LEED (76) work on Pd(111) that has placed the CO associated with the 1990 cm^{-1} peak in threefold hollow sites. Two reports suggest that the 1990 cm^{-1} peak is due to bridging CO adsorbed on edge sites (63, 77). A recent TLEED report has assigned a 1990 cm^{-1} peak to atop sites on Pd(110) (78). Assignments of threefold hollow adsorption, exclusive of the photoelectron diffraction and LEED work on Pd(111) (74–76), are limited to vibrational frequencies below 1880 cm^{-1} and usually appear only either in the presence of background CO (67, 70, 72) or at very low CO coverages (79). This lack of agreement regarding the 1990 cm^{-1} peak will have no impact on the outcome of this work. For the sake of clarity it will, in this work, be associated with 2-fold bridging CO.

The peak near 1925 cm^{-1} in Fig. 4—it only appears in CO vibrational data reported for supported palladium (41, 62–67, 80, 81)—falls in the lower end of the region assigned to bridge-bonded CO and grows in intensity with thermal processing. Since this growth continues after the peak at 2110 cm^{-1} is attenuated, the new state must have as its precursor the state associated with the peak at 1990 cm^{-1}. Based on the similarity of these results with those of the previously discussed "atop bent" adsorbed methylisocyanide mode, this peak is a candidate for assignment to an atop bound CO adsorbate mode displaying lifted backbond degeneracy **(III)**. Its appearance on supported palladium and not flat single-crystal surfaces (70, 72) seems to indicate its association with step or edge sites (81). No clear isosbestic point is evident in Fig. 4 as it was for the methylisocyanide data (Fig. 2), but the dipole-induced peak shifting of the 1990 cm^{-1} peak caused by its thermal depopulation could be obscuring it (Fig. 4) (38, 39).

This thermal activation of the peak at 1925 cm^{-1} has not been reported previously for CO on supported Pd (41, 62–66, 80, 81). Now that it has, suggested by the model methylisocyanide adsorption study, previous assignments of this peak to conventional CO bonding modes no longer seem tenable. One group assigns the peak to bridge bonding on terrace sites (63, 77) but that does not seem like a mode that would be thermally populated (Fig. 4) (79, 82). Assignment of the peak to a bridging site on the less prevalent (100) plane of the Pd crystallites (63, 83, 84) would be satisfactory based on peak position alone (79, 82), but those sites are known to be populated at low temperature (82). Arguing that the atop-bound CO (peak at 2110 cm^{-1}) could be blocking the (100) bridge sites at low temperature is likewise unreasonable since CO adsorption at 80 K on Pd(100) shows no atop adsorption (82). Atop-bound CO is detected on Pd(111) at low temperature (85) and so could block the bridging sites, but inspection of Fig. 4 reveals the peak associated with the atop-bound CO to be gone before the 1925 cm^{-1} peak has reached maximum intensity. Assignment of the peak to bridging CO on edge sites would likewise not seem reasonable since the work of Smulokowski (42, 86, 87), as interpreted by Sheu, *et al.* (81), and the work of Tersoff and Falicov (88) indicate that edge sites are electron poor and so should offer less backbonding electron density than found on terraces. This would mean at least a smaller red shift relative to the

bridging CO peak at 1990 cm^{-1} rather than the larger red shift seen in the data (Fig. 4). The claimed peak position for threefold bound CO on Pd(111) (70, 72) falls below 1880 cm^{-1}.

That the edge adsorbed bridging CO might somehow change the electronics of the edge and find a way to draw enough electron density from the edge to match the experimentally determined red shift is unlikely based on the variety of CO vibrational spectra collected on all surfaces (46, 47). If CO could dictate its degree of backbonding, then all of those spectra would be likely be identical.

Certain reports (62, 73) for CO on supported Pd in fact seem consistent with assigning the 1925 cm^{-1} peak to an atop mode. Both studies involve CO adsorption at 300 K on Pd surfaces where the bridging sites are disrupted either by partial oxidation of the Pd (62) or by dilution with Ag (73). CO vibrational peaks that are likewise disrupted under these conditions are believed associated with bridging surface states. In both cases the peak near 1990 cm^{-1} is depleted while the peak near 2100 cm^{-1} is enlarged, consistent with previous assignments of bridge- and atop-bound CO, respectively. However, in both cases (62, 73) a peak near 1925 cm^{-1} remains after the peak near 1990 cm^{-1} is gone. Since bridge bonding is unlikely for that state, atop bonding would seem to be indicated.

3. Assignment of 1925 cm^{-1} CO peak by qualitative arguments. The qualitative observations mentioned above for the adsorbate state associated with the peak at 1925 cm^{-1} are summarized in the following points:

1. The CO adsorbate state is likely bound to an atop site (62, 73).
2. The new CO adsorbate state is thermally stable (Fig. 4).
3. The CO adsorbate state is associated with edge sites since the associated peak is seen only on supported metals (41, 62–67, 80, 81).
4. The 1925 cm^{-1} peak does not shift to higher frequency as it grows with increasing temperature even though the 1990 cm^{-1} peak shifts to lower frequency as it attenuates (Fig. 4).
5. The CO adsorbate state is thermally activated (Fig. 4).
6. Not all of the adsorbed CO converts to the new state with heating (Fig. 4).
7. The analogously behaved peak associated with the atop-bent model methylisocyanide adsorbate is associated with lifted backbond degeneracy (Section IV.D.1).

Even before considering the analogy to methylisocyanide adsorption (point 7), interpretation of the qualitative adsorption data for CO on Pd (points 1–6) indicates much about the nature of the state associated with the 1925 cm^{-1} peak. First, its suggested association with an atop site (point 1) (62, 73) is strengthened by the above-described inability to assign the peak to a bridging site. Point 2, describing the peak's obvious thermal stability (Fig. 4), would then argue that its bonding mode would have to be somehow different from the atop mode associated with the peak at 2110 cm^{-1} which has little thermal stability (Fig. 4).

That the peak is associated with edge sites (point 3) is corroborated by observations other than the fact that the peak is seen only on supported metals (41, 62–67, 80, 81). First, point 4 summarizes how the peak's dipole coupling-induced shifting differs from that of the peak at 1990 cm^{-1} which moves to lower energy as it is depopulated by thermal processing. The 1925 cm^{-1} peak seems to move either to lower energy or remain stationary as its intensity grows. This is consistent with edge bonding since edges are one dimensional and adsorbate molecules arranged along that one dimension would create the same dipole field as would adsorbate molecules (i.e., those assigned to the 1990 cm^{-1} peak) located in two-dimensional arrays on the flat terraces (41, 68–73).

Second, association of the 1925 cm^{-1} peak with an edge site is consistent with the reported electron deficiency of edges as described by the work of Smulokowski (42, 86, 87), as interpreted by Sheu *et al.* (81), and the work of Tersoff and Falicov (88). The activation barrier for the conversion (point 5) could then be explained since CO molecules in the precursor bridging CO state (peak at 1990 cm^{-1}) on the electron-rich terraces would have to suffer a loss of backbonding electron density if they were to migrate toward the electron-poor edges. This migration, therefore, would require the input of energy.

This electron deficiency of edge metal atoms (42, 81, 86–88) also reveals the only likely source of the negative ΔH required to drive forward the conversion reaction of bridging CO to the new state. Since only some of the bridging CO converts to the new state (point 6), and only over a wide temperature range, the negative ΔH cannot arise through the transformation and stabilization of internal CO bonds. If only energy within CO bonds were released in this reaction, all CO molecules would convert to the more stable condition within a narrow temperature range regardless of how they were attached to the surface. Since this is not the case (Fig. 4), the negative ΔH must arise from the release of energy from other bonds.

The only bonds remaining in the system are those between the metal atoms themselves. Search of the surface for unstable metal atoms, atoms that would want to modify their metal-to-metal bonds to increase their stability, leads only to the electron-deficient atoms found on edges (42, 86–88) since basic thermodynamics requires that they also have a higher energy in a vacuum. These electron-deficient edge atoms would, therefore, be seeking a lower-energy condition than that which the band structure can provide to them. Since they can get it only by replacing bonds between metal atoms (band structure) with bonds to adsorbate molecules, a clear energy benefit exists for the association of this CO adsorbate state with edge sites. This edge atom instability

could even be large enough to drive the structure of the attached CO adsorbate molecule to a higher-energy condition to allow the metal atom to minimize its bonding to the metal band structure by maximizing its bonding to the CO adsorbate.

Since this source of negative ΔH is not dependent on adsorbate, it is, therefore, not unreasonable to conclude that the thermally activated "atop bent" methylisocyanide mode is also formed on edge sites. The changes in its molecular structure with conversion can be excluded as the source of the negative ΔH since, again, this conversion takes place over a wide temperature range in which the precursor and product adsorbate structures coexist. This again leaves only the edge atoms as the source of the negative ΔH.

The last question to answer is whether we can conclude that the atop edge-bound CO state displays the same lifted backbond degeneracy condition as the atop edge-bound, isoelectronic (21), methylisocyanide mode. The answer seems to be yes given that other conceivable CO adsorbate states do not seem to be consistent with the data. Side-on bound CO has not yet been reported in organometallic compounds (8) and is unlikely to ever be based on its large dipole moment that would destabilize side-on bonding. Atop-bound CO that donates electron density from its π bonds to adjacent metal centers is known (8), but its formation is not likely to require the energy released by edge atoms separating from the surface band structure. Oxygen-to-metal CO bonding is known only for CO already bound through the carbon atom (8).

With no other likely possibilities, the peak at 1925 cm^{-1} can be considered highly likely to be associated with a CO adsorbate state that is attached to a localized atop edge atom with an orbital structure that displays lifted backbond degeneracy. Figure 7 illustrates the structure of this proposed edge adsorbed CO state. The metal atom that is separated from the surface band structure and attached to the CO molecule can be seen as becoming part of the adsorbate. This would mean that the "Pd=C=O" complex would likely behave like any adsorbate and this may include some degree of surface mobility. While a good deal of consideration has been given to the issue of adsorbate-induced restructuring of surfaces (89), to our knowledge no suggestion has previously been made that the restructuring is driven by the separation of a metal atom from the destabilizing band structure.

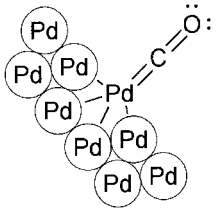

FIG. 7. Illustration of proposed atop CO bonding mode with lifted backbond degeneracy suggested for the edge sites on Pd/Al_2O_3. The absence of a circle around the Pd atom doubly bonded to the CO molecule represents its separation from the surface band structure and transformation into an adsorbate atom. The tilt is used to represent an edge.

E. Correlation with Published Data

If the proposed CO adsorbate state with lifted backbond degeneracy (Fig. 7) has actually been detected, then it should be possible to incorporate it into a discussion of data previously reported for CO adsorption on Pd surfaces. Although thermal processing data above 300 K (42, 57–61, 90), as mentioned above, are rare in the literature, studies of CO adsorbed on single-crystal Pd surfaces whose structures model edge sites, such as Pd(110) (69, 78, 91–94), or corner sites, such as Pd(210) (61, 79), and so likely contain electron-deficient surface atoms (42, 81, 86–88), offer some interesting possibilities.

Most significant is a report (78) of a TLEED study of the (2×1)CO overlayer on the corrugated Pd(110) surface that reports an on-top CO adsorbate state attached to top row metal atoms that are displaced from their clean surface positions. This exactly matches the conclusion drawn above through consideration of the qualitative observations of CO adsorbed on Pd. The authors (78) do not suggest why the atop-bound state appears, or why a displacement of the surface metal atoms might arise, but the above interpretation of an unstable metal atom isolating itself from the band structure through tight bonding to an adsorbed CO state does so handily.

This TLEED (78) result is contradicted by a photoelectron diffraction study (69) and HREELS studies (95, 96) of the (2×1)CO overlayer on Pd(110) that report bridging CO. A theoretical study (17) also favored bridging CO and investigations of CO on Ni(110) (97, 98) also contradict this result by claiming a bridging CO overlayer. However, these contradictory studies were conducted at *low* temperature where the (2×1) overlayer is known to be stable (99) [the theoretical study (17) did not include the surface reconstruction]. Since the TLEED study (78) did not report a sample temperature, and since the phase transition to a (4×2) overlayer is known to occur near 330 K (99), the TLEED study (78) might have been accidentally carried out on the so far uncharacterized (4×2) thermally activated overlayer. In addition, an IRAS study of CO adsorption on Pd(110) (90) between 180 and 305 K clearly shows a peak near 1915 cm^{-1} grow with heating and dominate the spectrum by 305 K, a temperature below the appearance of the (4×2) overlayer. Since the frequency of this thermally activated peak is close to that of the thermally activated peak in Fig. 4, it is possible that the conversion to the lifted backbond degeneracy state occurs on Pd(110) at a temperature below that of the phase change and so could lead to

confusion when LEED analyses are carried out at temperatures near that of the phase change. A lone HREELS study (100) of CO on Ni(110) also claims atop-bound CO and could have suffered from a similar situation.

Reports (92, 101) that adsorbed CO induces the reconstruction of the Pd(110) surface also are consistent with a lifted backbond degeneracy CO adsorbate state. If, as suggested above, the attached metal atom becomes part of the adsorbate, then it is likely that these "Pd=C=O" adsorbate complexes would become mobile on the surface, as is the case for most adsorbates, and seek out a more stable surface condition through surface reconstruction. Also, oscillating reactions (102, 103) on Pd may involve CO states with lifted backbond degeneracy since they also seem to be associated with surface reconstruction.

Examination of CO adsorption on the Pd(210) surface (79) offers additional insights but of an indirect sort. On Pd(210) the atoms in the top layer are too widely spaced for stable bridge bonding and, so, model corner sites that likely display an electron deficiency at least as large as that of edge sites (42, 81, 86–88). Since CO adsorption on Pd(210) at 300 K leads to vibrational peaks in the bridging region (79), they might be assigned to an atop CO state with lifted backbond degeneracy bound to the isolated top-layer Pd atoms. In fact, they are assigned to bridge bonded CO bound between atoms of the top two substrate layers (79) and ESDIAD corroborates this assignment at 300 K (61).

No vibrational or ESDIAD data are, however, presented to show what happens to these bridging CO adsorbate molecules when they are heated to above 300 K. Only the TPD data are available and show two widely spaced desorption peaks above 300 K at high coverage even though only two very similar bridging states are reported at 300 K (61). In the absence of thermal processing vibrational data above 300 K, it must therefore be considered possible that another bonding mode of CO adsorbed on Pd(210) might be thermally activated above 300 K prior to desorption to account for one of the two widely spaced desorption peaks. The possibility that it is the lifted backbond degeneracy CO state forming on the isolated top layer atoms cannot be excluded by the available data. If it were to form on Pd(210) it would be associated with the highest temperature desorption peak because of its stronger connection to the surface metal atom. Similar TPD data have been collected for CO adsorption on Pd(100) (82, 104).

On surfaces other than palladium, adsorbed CO may also bond through lifted backbond degeneracy **(III)**. TPD data for adsorbed CO on Ir(111) (58) [only atop-bound CO is detected by IRAS at 300 K (58)] show a similar doublet of broad TPD peaks centered around 420 and 500 K; a small shoulder is also seen below 400 K. These three TPD peaks for Ir(111) are assigned to surface coverages of atop bound CO that display three different degrees of lateral interaction (58). However, this assignment was made for the Ir(111) system through a Monte-Carlo calculation that required numerous assumptions (58), and, since iridium has a tendency to disfavor bridge-bonded CO (105), and since vibrational data were collected only up to 370 K (58), it is impossible to rule out the possibility that above 370 K some of the atop-bound CO molecules could have undergone a lifting of their backbond degeneracies to allow their attached surface Ir atoms to separate from the surface band structure and so lead to the higher-energy thermal desorption state.

This hypothesis is strengthened when considering the analogous CO TPD data for the Ir(110) surface (106). It shows a similar array of peaks that are also assigned to atop CO based on IRAS data (106). But the highest-temperature peak desorbs 100 K to higher temperature relative to its analog in the Ir(111) data (58) and it is difficult to imagine why atop-bound CO would behave so differently from one Ir surface to another. However, the assumption that the desorbing CO first converts to a lifted backbond degeneracy state, which would be bound more tightly to the Ir(110) surface, is completely consistent with this reported data.

But if adsorbed CO could assume a lifted backbond degeneracy state on the flat Ir(111) surface, that would imply a driving force for conversion based on a phenomenon other than the electron deficiency of edges (42, 81, 86–88). The slightly higher energy of surface atoms relative to bulk atoms could be the source of this requisite instability since there have been several reports (107–112) of flat single-crystal surfaces showing thermally activated CO peaks below 300 K that decay with cooling. This metastability is consistent with slightly unstable surface atoms bound to CO separating somewhat from the band structure at elevated temperature in a low-energy equilibrium process.

With the identification of this new edge bonding mode of CO on Pd, a great many further areas of investigation would seem to be opened. These would include the further thermal characterization, below and above 300 K, of adsorbed CO and methylisocyanide on surfaces that contain electron-deficient surface atoms (42, 81, 86–88). A "warm and hold" method of thermal treatment above 300 K would be particularly informative for overlayers on flat surfaces [i.e., Ir(111)] whose metal atoms show lesser degrees of instability. Future calculations regarding energy states and diffraction data might include adsorbate states with bond lengths and angles reflecting the lifted backbond degeneracy state and allow for the possibility of surface metal atom localization and mobility on adsorption. Consideration that diatomics with lifted backbond degeneracy could be involved in heterogeneous catalytic reactions would also be appropriate and the design of future catalysts could focus on optimizing edge density or preparation of distinct edges with a variety of surface atom instabilities for specific applications.

V. CONCLUSION

Qualitative analysis of transmission infrared data for thermally processed CO and methylisocyanide overlayers on Pd/Al_2O_3 in conjunction with literature reports indicates that a new atop bonding mode of CO is thermally prepared on the edge sites of supported Pd crystallites. Its characteristics are similar to those of the "atop bent" state of adsorbed methylisocyanide on the same surface in which the degeneracy of its backbonds is lifted. The data indicate that this state is formed so that electron-deficient, i.e., unstable, edge Pd atoms can maximize their stability by replacing bonds within the surface band structure with more stable bonds to the CO adsorbate.

Transmission infrared analysis indicates that methylisocyanide adsorbs on Pd/Al_2O_3 in the "atop linear," "bridge linear," and "atop bent" modes based on the correlation of ν(CN) stretching frequencies of the overlayer with those of bonding modes of methylisocyanide ligands found in metal complexes. The "atop bent" mode, known to display lifted backbond degeneracy, is a thermally activated state with a ν(M=C=N) asymmetric stretch mode on the low-energy side of the "bridge linear" adsorbate state. The vibrational peak for the thermally activated CO state on the same surface shares this behavior.

ACKNOWLEDGMENTS

I gratefully acknowledge the support of this work by John T. Yates, Jr., and the University of Pittsburgh Surface Science Center, the 3M Science Research Laboratory, and the 3M Corporate Research Laboratory. I especially acknowledge the comments and support of Alan Seidle of the 3M Corporation. Helpful discussions with Hans-Joachim Freund, Thomas P. Beebe, Jr., and Larry G. Sneddon are also appreciated.

REFERENCES

1. Gates, B. C., "Catalytic Chemistry." Wiley, New York, 1992.
2. Hoffmann, F. M., and Dwyer, D. J., *in* "Surface Science of Catalysis" (D. J. Dwyer and F. M. Hoffmann, Eds.), p. 1. Am. Chem. Soc., Washington, DC, 1992.
3. Satterfield, C. N., "Heterogeneous Catalysis in Practice." McGraw–Hill, New York, 1991.
4. Boudart, M., and Mariadassou, G. D., "Kinetics of Heterogeneous Catalytic Reactions." Princeton Univ. Press, Princeton, NJ, 1984.
5. Bond, G. C., "Heterogeneous Catalysis: Principles and Appliations." Clarendon Press, Oxford, 1987.
6. Worley, S. D., Wey, J. P., and Neely, W. C., *in* "Surface Science of Catalysis" (D. J. Dwyer and F. M. Hoffmann, Eds.), p. 250. Am. Chem. Soc., Washington, DC, 1992.
7. Bell, A. T., and Hegedus, L. L. (Eds.), "Catalysis under Transient Conditions." Am. Chem. Soc., Washington, DC, 1982.
8. Cotton, F. A., and Wilkinson, G., "Advanced Inorganic Chemistry," 5th ed. Wiley, New York, 1988.
9. Albert, M. R., and Yates, J. T., Jr., "The Surface Scientist's Guide to Organometallic Chemistry." ACS Books, Washington, DC, 1987.
10. Nilsson, A., Wassdahl, N., Weinelt, M., Karis, O., Wiell, T., Bennich, P., Hasselström, J., Föhlisch, A., Stöhr, J., and Samant, M., *Appl. Phys. A* **65**, 147 (1997).
11. Nilsson, A., Weinelt, M., Wiell, T., Bennich, P., Karis, O., and Wassdahl, N., *Phys. Rev. Lett.* **78**, 2847 (1997).
12. Rösch, N., Sandl, P., Knappe, P., Görling, A., and Dunlap, B. I., *Z. Phys. D* **12**, 547 (1989).
13. Kuhlenbeck, H., Neumann, M., and Freund, H.-J., *Surf. Sci.* **173**, 194 (1986).
14. Pacchioni, G., Chung, S.-C., Krüger, S., and Rösch, N., *Surf. Sci.* **392**, 173 (1997).
15. Illas, F., Zurita, S., Márquez, A. M., and Rubio, J., *Surf. Sci.* **376**, 279 (1997).
16. Persson, B. N. J., Tüshaus, M., and Bradshaw, A. M., *J. Chem. Phys.* **92**, 5034 (1990).
17. Hu, P., King, D. A., Crampin, S., Lee, M.-H., and Payne, M. C., *Chem. Phys. Lett.* **230**, 501 (1994).
18. Herman, R. (Ed.), "Catalytic Conversions of Synthesis Gas and Alcohols to Chemicals." Plenum, New York, 1984.
19. Coulston, G. W., Haller, G. L., *in* "Surface Science of Catalysis" (D. J. Dwyer and F. M. Hoffmann, Eds.), p. 58. Am. Chem. Soc., Washington, DC, 1992.
20. Bassett, J.-M., Berry, D. E., Barker, G. K., Green, M., Howard, J. A. K., and Stone, F. G. A., *J. Chem. Soc. Dalton*, 1003 (1979).
21. Cavanaugh, R. R., and Yates, J. T., Jr., *J. Chem. Phys.* **75**, 1551 (1981).
22. Semancik, S., Haller, G. L., and Yates, J. T., Jr., *J. Chem. Phys.* **78**, 6970 (1983).
23. Szilagyi, T., *Appl. Surf. Sci.* **35**, 19 (1988–1989).
24. Avery, N. R., and Matheson, T. W., *Surf. Sci.* **143**, 110 (1984).
25. Friend, C. M., Muetterties, E. L., and Gland, G. L., *J. Phys. Chem.* **85**, 3256 (1981).
26. Avery, N. R., Matheson, T. W., and Sexton, B. A., *Appl. Surf. Sci.* **22/23**, 384 (1985).
27. Ceyer, S. T., and Yates, J. T., Jr., *J. Phys. Chem.* **89**, 3842 (1985).
28. Friend, C. M., Stein, J., and Muetterties, E. L., *J. Am. Chem. Soc.* **103**, 767 (1981).
29. Hickman, J. J., Zou, C., Ofer, D., Harvey, P. D., and Wrighton, M. S., *J. Am. Chem. Soc.* **111**, 7271 (1989).
30. Ontko, A. C., and Angelici, R. J., *Langmuir* **14**, 1684 (1998).
31. Hoffmann, R., Chen, M. M.-L., and Thorn, D. L., *Inorg. Chem.* **16**, 503 (1977).
32. Hoffmann, R., "Solids and Surfaces: A Chemist's View of Bonding in Extended Structures." VCH, New York, 1988.
33. Muetterties, E. L., Rhodin, T. N., Band, E., Brucker, C. F., and Pretzer, W. R., *Chem. Rev.* **79**, 91 (1979).
34. Bradshaw, A. M., *Surf. Sci.* **331–333**, 978 (1995).
35. Pasto, D. J., and Johnson, C. R., "Organic Structure Determination." Prentice–Hall, London, 1969.
36. Yates, J. T., Jr., Duncan, T. M., Worley, S. D., and Vaughn, R. W., *J. Chem. Phys.* **70**, 1219 (1979).
37. Casanova, J., Schuster, R. E., and Werner, N. D., *J. Chem. Soc.* 4280, (1963).
38. Hollins, P., and Pritchard, J., *in* "ACS Symposium Series" (A. T. Bell and M. L. Hair, Eds.), Vol. 137, p. 51. Am. Chem. Soc., Washington, DC, 1980.
39. Hayden, B. E., *in* "Vibrational Spectroscopy of Molecules on Surfaces" (J. T., Yates Jr., and T. E. Madey, Eds.), p. 317. Plenum, New York, 1987.
40. Beebe, T. P., Jr., and Yates, J. T., Jr., *Surf. Sci.* **173**, L606 (1986).
41. Gelin, P., Seidle, A. R., and Yates, J. T., Jr., *J. Phys. Chem.* **88**, 2978 (1984).
42. Yates, J. T., Jr., *J. Vac. Sci. Technol. A* **13**, 1359 (1995).
43. Singleton, E., and Oosthuizen, H. E., *Adv. Organomet. Chem.* **22**, 209 (1983).
44. Sutton, D., *Chem. Soc. Rev.* **4**, 443 (1975).
45. Treichel, P. M., *Adv. Organomet. Chem.* **11**, 21 (1972).

46. Campuzano, J. C., *in* "The Chemical Physics of Solid Surfaces and Heterogeneous Catalysis" (D. A. King and D. P. Woodruff, Eds.), Vol. 3, Part A, p. 389. Elsevier, Amsterdam, 1990.
47. Yates, J. T., Jr., *Surf. Sci.* **299/300**, 731 (1994).
48. Hwang, S. Y., Seebauer, E. G., and Schmidt, L. D., *Surf. Sci.* **188**, 219 (1987).
49. Chen, J. J., and Winograd, N., *Surf. Sci.* **326**, 285 (1995).
50. Kordesch, M. E., Stenzel, W., and Conrad, H., *Surf. Sci.* **175**, L687 (1986).
51. Ratliff, K. S., Broeker, G. K., Fanwick, P. E., and Kubiak, C. P., *Angew. Chem. Int. Ed. Engl.* **29**, 395 (1990).
52. Eischens, R. P., Francis, S. A., and Pliskin, W. A., *J. Phys. Chem.* **60**, 194 (1956).
53. Kniseley, R. N., Hirschman, R. P., and Fassel, V. A., *Spectrochim. Acta. A* **23**, 109 (1967).
54. Durig, J. R., Sullivan, J. F., Heusel, H. L., and Cradock, S. J., *Mol. Struct.* **100**, 241 (1983).
55. Franklin, W. J., Werner, R. L., and Ashby, R. A., *Spectrochim. Acta. A* **30**, 1293 (1974).
56. Peaks in both the ν(C–H) and $\delta(CH_3)$ spectral regions were collected along with the reported ν(CN) data. While a complete analysis of those data is beyond the requirements of this work, their interpretation is consistent with the stated conclusions even though an earlier work (113) reports difficulty detecting the ν(C–H) peaks of surface methyl groups on Pd/Al_2O_3. .
57. Luo, J. S., Tobin, R. G., Lambert, D. K., Fisher, G. B., and DiMaggio, C. L., *J. Chem. Phys.* **99**, 1347 (1993).
58. Lauterbach, J., Boyle, R. W., Schick, M., Mitchell, W. J., Meng, B., and Weinberg, W. H., *Surf. Sci.* **350**, 32 (1996); erratum: **366**, 228 (1996).
59. Xu, J., and Yates, J. T., Jr., *J. Chem. Phys.* **99**, 725 (1993).
60. Luo, J. S., Tobin, R. G., Lambert, D. K., Fisher, G. B., and DiMaggio, C. L., *Surf. Sci.* **274**, 53 (1992).
61. Madey, T. E., Yates, J. T., Jr., Bradshaw, A. M., and Hoffmann, F. M., *Surf. Sci.* **89**, 370 (1979).
62. Palazov, A., Chang, C. C., and Kokes, R. J., *J. Catal.* **36**, 338 (1975).
63. Wolter, K., Seiferth, O., Kuhlenbeck, H., Bäumer, M., and Freund, H.-J., *Surf. Sci.* **399**, 190 (1998).
64. Rainer, D. R., Xu, C., Holmblad, P. M., and Goodman, D. W., *J. Vac. Sci. Technol. A* **15**, 1653 (1997).
65. Xu, X., and Goodman, D. W., *J. Phys. Chem.* **97**, 7711 (1993).
66. Rainer, D. R., Wu, M.-C., Mahon, D. I., and Goodman, D. W., *J. Vac. Sci. Technol. A* **14**, 1184 (1996).
67. Almusaiteer, K., and Chuang, S. C., *J. Catal.* **180**, 161 (1998).
68. Conrad, H., Ertl, G., Kock, J., and Latta, E. E., *Surf. Sci.* **43**, 462 (1974).
69. Locatelli, A., Brena, B., Lizzit, S., Comelli, G., Paulucci, G., and Rosei, R., *Phys. Rev. Lett.* **73**, 90 (1994).
70. Szanyi, J., Kuhn, W. K., and Goodman, D. W., *J. Vac. Sci. Technol. A* **11**, 1969 (1993).
71. Xu, X., Szanyi, J., Xu, Q., and Goodman, D. W., *Catal. Today* **21**, 57 (1994).
72. Xu, X., and Goodman, D. W., *Catal. Lett.* **24**, 31 (1994).
73. Soma-Noto, Y., and Sachtler, W. M. H., *J. Catal.* **32**, 315 (1974).
74. Fernandez, V., Gießel, T., Schaff, O., Schindler, K.-M., Theobald, A., Hirschmugl, C. J., Bao, S., Bradshaw, A. M., Baddeley, C., Lee, A. F., Lambert, R. M., Woodruff, D. P., and Fritsche, V., *Z. Phys. Chem.* **198**, 73 (1997).
75. Gießel, T., Schaff, O., Hirschmugl, C. J., Fernandez, V., Schindler, K.-M., Theobald, A., Bao, S., Lindsay, R., Berndt, W., Bradshaw, A. M., Baddeley, C., Lee, A. F., Lambert, R. M., and Woodruff, D. P., *Surf. Sci.* **406**, 90 (1998).
76. Ohtani, H., Van Hove, M. A., and Somorjai, G. A., *Surf. Sci.* **187**, 372 (1987).
77. Wolter, K., Seiferth, O., Libuda, J., Kuhlenbeck, H., Bäumer, M., and Freund, H.-J., *Surf. Sci.* **402–404**, 428 (1998).
78. Wander, A., Hu, P., and King, D. A., *Chem. Phys. Lett.* **201**, 393 (1993).
79. Bradshaw, A. M., and Hoffmann, F. M., *Surf. Sci.* **72**, 513 (1978).
80. Baddour, R. F., Modell, M., and Goldsmith, R. L., *J. Phys. Chem.* **74**, 1787 (1970).
81. Sheu, L.-L., Karpinski, Z., and Sachtler, W. M. H., *J. Phys. Chem.* **93**, 4890 (1989).
82. Ortega, A., Hoffman, F. M., and Bradshaw, A. M., *Surf. Sci.* **119**, 79 (1982).
83. Burwell, R. L., Jr., *Langmuir* **2**, 2 (1986).
84. van Hardeveld, R., and Hartog, F., *Surf. Sci.* **15**, 189 (1969).
85. Tüshaus, M., Berndt, W., Conrad, H., Bradshaw, A. M., and Persson, B., *Appl. Phys. A* **51**, 91 (1990).
86. Gomer, R., "Field Emission and Field Ionization." Harvard Univ. Press, Cambridge, MA, 1961.
87. Smoluchkowski, R., *Phys. Rev.* **60**, 661 (1941).
88. Tersoff, J., and Falicov, L. M., *Phys. Rev. B* **24**, 754 (1981).
89. Somorjai, G. A., and Van Hove, M. A., *Prog. Surf. Sci.* **30**, 201 (1989).
90. Fukui, K., Miyauchi, H., and Iwasawa, Y., *J. Phys. Chem.* **100**, 18,795 (1996).
91. Raval, R., Harrison, M. A., and King, D. A., *Surf. Sci.* **211/212**, 61 (1989).
92. Raval, R., Haq, S., Harrison, M. A., Blyholder, G., and King, D. A., *Chem. Phys. Lett.* **167**, 391 (1990).
93. Fukui, K., Miyauchi, H., and Iwasawa, Y., *J. Phys. Chem.* **100**, 18,795 (1996).
94. Raval, R., Blyholder, G., Haq, S., and King, D. A., *J. Phys. Condens. Matter* **1**, SB165 (1989).
95. Kato, H., and Kawaii, M., *Phys. Rev. Lett.* **82**, 1899 (1999).
96. Kato, H., Yoshinobu, J., and Kawai, M. *Surf. Sci.* **427/428**, 69 (1999).
97. Pangher, N., and Haase, J., *Surf. Sci.* **293**, L908 (1993).
98. Haung, Z., Hussain, Z., Huff, W. T., Moler, E. J., and Shirley, D. A., *Phys. Rev. B* **48**, 1696 (1993).
99. He, J.-W., and Norton, P. R., *J. Chem. Phys.* **89**, 1170 (1988).
100. Voightländer B., Bruchmann, D., Lehwald, S., and Ibach, H., *Surf. Sci.* **225**, 151 (1990).
101. Hu, P., Morales de la Garza, L., Raval, R., and King, D. A., *Surf. Sci.* **249**, 1 (1991).
102. Ladas, S., Imbihl, R., and Ertl, G., *Surf. Sci.* **198**, 42 (1980).
103. Schwartz, S. B., and Schmidt, L. D., *Surf. Sci.* **183**, L269 (1987).
104. Behm, R. J., Christmann, K., Ertl, G., and Van Hove, M. A., *J. Chem. Phys.* **73**, 2984 (1980).
105. Deeming, A. J., *Adv. Organomet. Chem.* **26**, 1 (1986).
106. Lyons, K. J., Xie, J., Mitchell, W. J., and Weinberg, W. H., *Surf. Sci.* **325**, 85 (1995).
107. Hayden, B. E., and Bradshaw, A. M., *Surf. Sci.* **125**, 787 (1983).
108. Hayden, B. E., Kretzschmar, K., and Bradshaw, A. M., *Surf. Sci.* **155**, 553 (1985).
109. Trenary, M., Uram, K. J., Bozso, F., and Yates, J. T., Jr., *Surf. Sci.* **146**, 269 (1984).
110. Yoshinobu, J., Takagi, N., and Kawai, M., *Phys. Rev. B* **49**, 16670 (1994).
111. Pfnür, H., Menzel, D., Hoffmann, F. M., Ortega, A., and Bradshaw, A. M., *Surf. Sci.* **93**, 431 (1980).
112. Schweizer, E., Persson, B. N. J., Tüshaus, M., Hoge, D., and Bradshaw, A. M., *Surf. Sci.* **213**, 49 (1989).
113. Beebe, T. P., Jr., and Yates, J. T., Jr., *J. Phys. Chem.* **91**, 254 (1987).